

Catalytic Contribution of Phenylalanine-101 of 3-Oxo- Δ^5 -steroid Isomerase[†]

Lin Qi and Ralph M. Pollack*

Laboratory for Chemical Dynamics, Department of Chemistry and Biochemistry, 1000 Hilltop Circle, University of Maryland, Baltimore County, Baltimore, Maryland 21250, and Center for Advanced Research in Biotechnology, 9600 Gudelsky Drive, Rockville, Maryland 20850

Received November 6, 1997; Revised Manuscript Received February 5, 1998

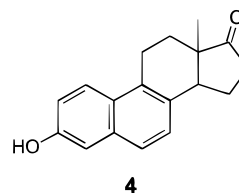
ABSTRACT: 3-Oxo- Δ^5 -steroid isomerase (KSI, EC 5.3.3.1) from *Pseudomonas testosteroni* catalyzes the isomerization of a variety of 3-oxo- Δ^5 -steroids to their conjugated Δ^4 -isomers through the formation of an intermediate dienolate ion. It has previously been found in our laboratory that the aromatic ring of Phe-101 is important for catalysis. The present work extends these studies. Two double-mutant KSIs (D38E/F101L and D38E/F101A) were prepared to compare the free energy profiles for the reactions catalyzed by these mutants and by D38E. Both double-mutant KSIs show reduced values of k_{cat} at pH 7 compared to D38E (~25-fold for D38E/F101L and ~200-fold for D38E/F101A), similar to the reduced values for F101L and F101A relative to KSI (~30-fold for F101L and ~270-fold for F101A). Free energy profiles for the reactions catalyzed by D38E/F101L and D38E/F101A indicate that the bound transition state(s) and bound intermediate are destabilized when the large aromatic residue Phe-101 in D38E KSI is replaced by the smaller residues Leu or Ala. The pH-rate profiles for D38E, D38E/F101L, and D38E/F101A in the pH range 3.9–8.7 show that the pK_a of the catalytic base (Glu-38) is perturbed. In addition, these mutants have significant catalytic activity in the low-pH region.

3-Oxo- Δ^5 -steroid isomerase (EC 5.3.3.1, Δ^5 -3-ketosteroid isomerase, KSI¹) from *Pseudomonas testosteroni* catalyzes the conversion of a variety of 3-oxo- Δ^5 -steroids to their conjugated Δ^4 -isomers (1–3). KSI is one of the most active enzymes known, with a k_{cat} of approximately $6 \times 10^4 \text{ s}^{-1}$ per monomer at pH 7 for 5-androstene-3,17-dione (4, 5). Numerous experiments have implicated Asp-38 and Tyr-14 as catalytically active residues (5–8), with Asp-38 transferring a proton from C-4 to C-6 and Tyr-14 polarizing the carbonyl by hydrogen bonding (9, 10). Recently, Wu et al. (11) determined the complete three-dimensional structure of KSI and showed that Asp-99 is also located in the active site. In addition, the carboxyl group of Asp-99 is positioned such that it could form a hydrogen bond to the substrate carbonyl, along with the hydrogen bond from Tyr-14. A reasonable mechanism in accord with the data is shown in Scheme 1.

The free energy profile for conversion of 5-androstene-3,17-dione (1) to 4-androstene-3,17-dione (3) by wild-type KSI has been determined (12, 13), along with the corresponding free energy profile for the model reaction catalyzed by acetate ion (14). The catalytic activity of KSI has been dissected into contributions from uniform binding, differential binding, and catalysis of elementary steps, and this analysis was used to rationalize the enzymatic rate acceleration (12).

A major function of the enzyme is to stabilize the bound dienolate ion (2), such that the equilibrium constant for the formation of 2 from 1 at the active site (K_{int}) is about unity. This value contrasts sharply with the corresponding equilibrium constant in aqueous solution (K_{ext}) of 10^{-8} . Stabilization of the intermediate is likely to be due primarily to the combination of hydrogen bonds from Tyr-14 and Asp-99 (11).

Recently, we found that when one of the phenylalanine residues in the active site of KSI (Phe-101) is replaced with either leucine or alanine, k_{cat} for the isomerization of 5-androstene-3,17-dione at pH 7 is reduced by ~30-fold (F101L) or ~270-fold (F101A) (15). Surprisingly, K_{m} values for the mutants are similar to K_{s} for wild type (WT) (12), suggesting that there is no significant interaction of the substrate with the side chain of Phe-101. Similarly, there is only a small change in the dissociation constant (≤ 4 -fold) for the product 4-androstene-3,17-dione with both mutants. However, these mutants bind the intermediate analogue *d*-equilenin (4) about 25-fold less tightly than does wild-type KSI (15). Using the binding of *d*-equilenin as a model for binding of the intermediate, free energy profiles for the reactions catalyzed by these mutants were constructed.



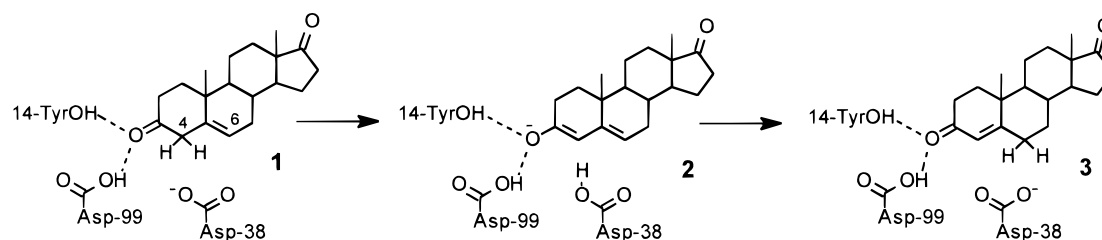
We have now extended these studies to the double mutants D38E/F101L and D38E/F101A. With these mutants, it is

[†] This work was supported by Grant GM 38155 from the National Institutes of Health.

* Address correspondence to this author at the University of Maryland, Baltimore County.

¹ Abbreviations: KSI, 3-oxo- Δ^5 -steroid isomerase; WT, wild-type KSI from *Pseudomonas testosteroni*; SDS, sodium dodecyl sulfate; PAGE, polyacrylamide gel electrophoresis; BSA, bovine serum albumin.

Scheme 1



possible to *directly* determine the energy of the bound intermediate, making it unnecessary to rely on an estimate based on an analogue. These results point to a role for the aromatic ring of Phe-101 in preferentially stabilizing the transition state(s) and, to a lesser extent, the intermediate, relative to the reactant and product. In addition, we determined the pH-rate profiles for the two double mutants and find that the pK_a of the catalytic base (Glu-38) is higher in the double mutants than in the single D38E mutant. Furthermore, there is significant activity at low pH, which is greater than that predicted from a simple titration of Glu-38.

MATERIALS AND METHODS

Materials. Restriction endonucleases, T4 DNA ligase, and the appropriate buffers were purchased from Promega Corporation. Reagents for plasmid isolation and purification were obtained from QIAGEN Inc. (QIAGEN plasmid midi kit). The reagents for the isolation and purification of the DNA fragments from agarose gels were purchased from BIO101, Inc., in the Gene Clean II Kit. 5-Androstene-3,17-dione (**1**) was synthesized by G. Blotny of this laboratory (15); 4-androstene-3,17-dione (**3**) content was estimated to be less than 5% on the basis of the absorbance at 248 nm prior to and after isomerization of **1** with KSI.

Preparation of Double-Mutant KSI Genes by Cassette (Deletion–Insertion) Mutagenesis. Plasmid DNAs were purified using the QIAGEN plasmid midi kit. DNA digestion and ligation procedures were based on those given by Sambrook et al. (16). The recombinant plasmids containing mutant KSI genes, including D38E (pUC18–KSI_{D38E}), F101A (pUC18–KSI_{F101A}), and F101L (pUC18–KSI_{F101L}), had been previously transformed into the *Escherichia coli* strains JM105 and NCM533 (13, 15, 17). Each of these plasmids was isolated and transformed into the *dam*[−] *E. coli* strain NF3079. Plasmids purified from these cells were cleaved with the restriction endonucleases *Cla*I and *Bam*HI. The DNA fragments were separated by agarose gel electrophoresis, cut from the gel, and purified according to the protocol of the Gene Clean II kit. Two DNA fragments were obtained from each single-mutant KSI recombinant plasmid. The large fragment, containing a substitution at 101 (F101L or F101A), and the small fragment, containing a substitution at position 38 (D38E), were ligated by T4 DNA ligase to form recombinant double-mutant plasmids containing D38E/F101X genes. Clones containing the correct size insert were identified by digestion with the restriction endonucleases *Eco*RI and *Hind*III. The entire KSI gene in each double-mutant plasmid was sequenced by the Biopolymer Laboratory, University of Maryland, Baltimore, to verify that only the expected mutations were present. The double-mutant

plasmids were transformed into *E. coli* strain NCM 533 (15), and the mutant enzymes were purified using methods described earlier (18). The concentration of each enzyme solution was determined by its UV absorbance at 280 nm, using an absorbance value of 0.336 for 1 mg/mL of KSI (19). Specific activities were determined under standard conditions (20).

Determination of the Kinetic Parameters. Steady-state kinetic parameters were determined by initial rate experiments as previously described (4). The reaction mixture contained 10–90 μ M 5-androstene-3,17-dione, 3.3% (v/v) methanol, and 100 μ g of bovine serum albumin (BSA) in 3.00 mL of potassium phosphate buffer at pH 7.0 or 7.6. Isomerization was initiated by adding 10 μ L of appropriately diluted KSI solution in 1% BSA and mixing for 10 s. The reaction was monitored at 248 nm for about 20% completion, and the initial linear reaction velocities were determined for 5% conversion of the substrate.

The partitioning of the enzyme-bound dienolate intermediate for mutant KSIs was determined as previously described for the D38E mutant (12, 18).

RESULTS

Preparation of Double-Mutant KSIs. The genes for the double-mutant KSIs D38E/F101L and D38E/F101A were prepared by cassette mutagenesis. Plasmid DNAs containing single-base substitutions corresponding to D38E, F101A, and F101L were isolated and cleaved by two restriction endonucleases, *Bam*HI and *Cla*I. The *Bam*HI restriction site is located in the multiple cloning site of pUC18 at the 5' end of the KSI gene insert, whereas the *Cla*I restriction site is located within the KSI gene between the two desired mutation positions, 38 and 101. Appropriate fragments containing mutations at positions 38 and 101 were ligated to form plasmids containing the double-mutant KSI genes. Each of these was transformed into *E. coli* strain NCM 533 for expression of the double-mutant protein. After purification, each mutant KSI showed a single band on SDS–PAGE. Specific activities were 2.0 (D38E/F101A) and 19 units/mg·min protein (D38E/F101L).

Determination of the Free Energy Profiles for D38E/F101L and D38E/F101A. The complete free energy profiles were determined by the method previously used for D38E (18), which involves the determination of the steady-state kinetic parameters for isomerization of **1**, the dissociation constants for **3**, and the partitioning of the reaction of an externally generated **2** with the enzyme. These experiments were all done in 330 mM phosphate, since the partitioning experiments require high concentrations of buffer (18).

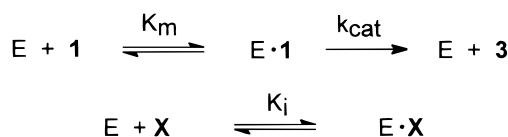
The steady-state kinetic parameters k_{cat} and K_m for the KSI mutants D38E/F101A and D38E/F101L were determined at

Table 1: Kinetic Constants for the Isomerization of 5-Androstene-3,17-dione (**1**) to 4-Androstene-3,17-dione (**3**) Catalyzed by D38E, D38E/F101L, and D38E/F101A^{a,b}

KSI	conditions	K_m (μ M)	k_{cat} (s^{-1})	k_{cat}/K_m ($M^{-1} s^{-1}$)
D38E	330 mM, pH 7.0 ^c	72 \pm 14	120 \pm 24	(1.7 \pm 0.2) $\times 10^6$
	34 mM, pH 7.0	80 \pm 7	120 \pm 8	(1.50 \pm 0.03) $\times 10^6$
	34 mM, pH 7.6	88 \pm 5	135 \pm 7	(1.53 \pm 0.04) $\times 10^6$
D38E/F101L	330 mM, pH 7.0	13.4 \pm 0.3	4.04 \pm 0.06	(3.0 \pm 0.1) $\times 10^5$
	330 mM, pH 7.6	61 \pm 6	20 \pm 1	(3.3 \pm 0.3) $\times 10^5$
	34 mM, pH 7.0	28 \pm 1	7.4 \pm 0.2	(2.6 \pm 0.1) $\times 10^5$
	34 mM, pH 7.6	48 \pm 4	16 \pm 1	(3.3 \pm 0.1) $\times 10^5$
D38E/F101A	330 mM, pH 7.0	9.4 \pm 0.4	0.42 \pm 0.01	(4.5 \pm 0.2) $\times 10^4$
	330 mM, pH 7.6	33 \pm 3	1.5 \pm 0.1	(4.4 \pm 0.4) $\times 10^4$
	34 mM, pH 7.0	13.1 \pm 0.8	0.59 \pm 0.05	(4.5 \pm 0.4) $\times 10^4$
	34 mM, pH 7.6	27 \pm 2	1.29 \pm 0.04	(4.8 \pm 0.2) $\times 10^4$

^a Potassium phosphate buffer and 3.3% MeOH, 25.0 °C. ^b Errors are standard deviations. ^c Reference 18.

Scheme 2

Table 2: Inhibition Constants (K_i) for the Product 4-Androstene-3,17-dione (**3**) and the Intermediate Analogue *d*-Equilenin (**4**) for the Isomerization of **1** to **3** Catalyzed by Wild-Type, D38E, D38E/F101L, and D38E/F101A KSI^{a,b}

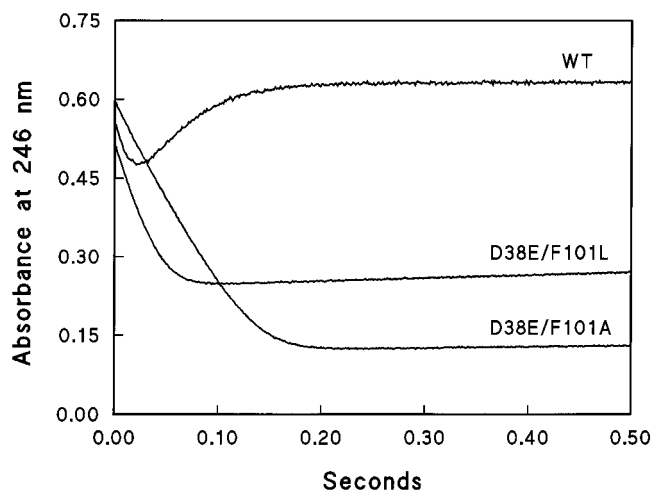
KSI	K_i (3) (μ M)	K_i (4) (μ M)
WT	148 \pm 30 ^c	2.7 \pm 0.7 ^d
D38E	61 \pm 12 ^c	0.77 \pm 0.17 ^d
D38E/F101L	22 \pm 2	2.4 \pm 0.1
D38E/F101A	15 \pm 2	0.69 \pm 0.02

^a Potassium phosphate buffer, 330 mM, 3.3% MeOH, pH 7.0, 25.0 °C. ^b Errors are standard deviations. ^c Reference 18. ^d Reference 13.

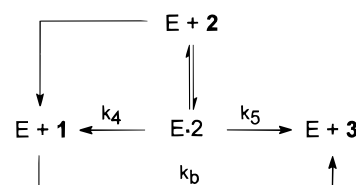
25.0 °C at pH 7.0 and 7.6. The kinetic constants k_{cat} and K_m calculated from weighted double-reciprocal plots are given in Table 1. With both mutants, k_{cat} is reduced from the corresponding value for D38E, by 16–30-fold for D38E/F101L, and by 200–300-fold for D38E/F101A at pH 7. The second-order rate constant k_{cat}/K_m is also substantially reduced with both double mutants (ca. 5-fold for D38E/F101L and ca. 35-fold for D38E/F101A).

Inhibition constants (K_i) for 4-androstene-3,17-dione (**3**) and the intermediate analogue *d*-equilenin (**4**) were determined by monitoring the complete time course of the enzymatic isomerization of **1** to **3** with varying initial concentrations of **1** (10–50 μ M) and **3** or **4** (0–50 μ M) at 25.0 °C in 330 mM phosphate buffer (pH 7.0). The data were then fit to the mechanism of Scheme 2 (with X = **3** or **4**), using the KINSIM/FITSIM programs (21, 22) to give inhibition constants for both **3** and **4** with D38E/F101A and D38E/F101L (Table 2). These data were used in the calculation of the free energy profiles at pH 7.6.

To determine the partitioning of the dienol intermediate at the enzyme active site, **2** was generated in situ in the stopped-flow spectrophotometer by mixing a solution of **1** with 1.0 N NaOH in a 1:1 ratio. At this concentration of base (0.5 N), the dienolate (**2**) is formed within milliseconds, but it reacts substantially more slowly to **3** (12). When this solution is quenched with an excess of buffer after a 0.5-s delay, a mixture of 12% of **1**, 83% of **2**, and 5% of **3** is obtained (12). If KSI is included in the quenching solution, the reaction of **2** with KSI can be monitored at the isosbestic

FIGURE 1: Absorbance change at 246 nm for the reaction of the independently generated dienol (**2**) with WT, D38E/F101A, and D38E/F101L in 330 mM potassium phosphate at 25.0 °C.

Scheme 3



wavelength for **2** and **3** (246 nm).² With WT KSI, a rapid decrease of absorbance due to the decomposition of **2** to a mixture of **1** and **3** is followed by a subsequent increase due to enzymatic conversion of **1** to **3** (Figure 1). The shapes of the curves for the reactions catalyzed by D38E/F101A and D38E/F101L are similar to that observed with D38E (18) and show saturation kinetics for the initial decomposition of **2**, with a much slower conversion of **1** to **3**. These data were fit to the mechanism of Scheme 3, using the KINSIM/FITSIM program (21, 22) to give rate constants for conversion from $E \cdot 2$ to **1** (k_4) and from $E \cdot 2$ to **3** (k_5) and the apparent dissociation constant for the complex of $E \cdot 2$ (K_m), shown in Table 3.

With these values in hand, the complete free energy profiles for the D38E/F101A and D38E/F101L mutants were

² The isosbestic wavelength was determined to be 246 nm, with an extinction coefficient of 15 200 $M^{-1} cm^{-1}$. Previous isosbestic wavelength determinations in our laboratory gave 243 (12) and 249.5 nm (18). Although the exact values differ, results using wild type at each of these wavelengths are identical.

Table 3: Rate Constants for the Reaction of Dienol (**2**) with D38E/F101L, D38E/F101A, and D38E^{a,b}

enzyme	1K_m (μ M)	k_4 (s^{-1})	k_5 (s^{-1})	$k_5/(k_4 + k_5)$ (%)
D38E ^c	2.0 ± 0.6	320 ± 30	335 ± 20	51
D38E/F101L	6.9 ± 0.3	245 ± 3.3	256 ± 3.0	51
D38E/F101A	1.5 ± 0.1	75 ± 0.6	6.3 ± 0.06	7.7

^a Potassium phosphate buffer, 330 mM, and 3.3% MeOH, pH 7.6, 25.0 °C. ^b Errors are standard deviations. ^c Reference 18.

calculated as before (18). These are shown in Figure 2, along with the corresponding profile for the D38E mutant. Microscopic kinetic constants are given in Table 4.

pH-Rate Profiles. The kinetic parameters k_{cat} and k_{cat}/K_m for the isomerization of **1** to **3** by D38E, D38E/F101A, and D38E/F101L were determined in the pH range 3.9–8.7 in 34 mM acetate (pH < 5.9) or phosphate (pH > 5.9) buffers at ionic strength 0.1 M and 25.0 °C (Figure 3). It is clear that the experimental data require a pathway leading to product at low pH, as well as near neutrality (Scheme 4). The pK_a 's for the free enzymes (pK_E) and the enzyme–substrate complexes (pK_{ES}) were calculated by least-squares fitting of $(k_{cat}/K_m)_{obs}$ and $(k_{cat})_{obs}$ to eqs 1 and 2, respectively, which are derived from Scheme 4. Excellent fits to these equations gave the values in Table 5.

$$(k_{cat}/K_m)_{obs} = \frac{(k_{cat} K_E/K_S + k_{cat}'[H^+]/K_S')/(K_E + [H^+])}{(k_{cat})_{obs} = (k_{cat} K_{ES} + k_{cat}'[H^+])/(K_{ES} + [H^+])} \quad (1)$$

$$(k_{cat})_{obs} = (k_{cat} K_{ES} + k_{cat}'[H^+])/(K_{ES} + [H^+]) \quad (2)$$

DISCUSSION

Catalytic Role of Phe-101. In previous work (15), we found that Phe-101 plays an important role in the catalytic mechanism of KSI. Thus, k_{cat} is substantially decreased relative to wild type (WT) for both the F101L (16–30-fold) and the F101A (200–300-fold) mutant at pH 7.0, although the K_m values vary by only a factor of about 2. In each case, the intermediate analogue equilenin (**4**) shows decreased affinity for the mutant enzyme relative to wild type by ca. 25-fold. The results are qualitatively similar when the kinetic constants of the D38E/F101L and D38E/F101A double mutants are compared with the D38E mutant. At pH 7.0, k_{cat} is lower for both double mutants by 15–30-fold (D38E/F101L) and 200–300-fold (D38E/F101A) compared to the single-mutant D38E. At pH 7.6, the ratios are somewhat smaller, but still substantial (8-fold and 100-fold, respectively).

In our work with the single mutants F101L and F101A (15), we were unable to accurately determine the complete free energy profiles. The internal equilibrium constants for interconversion of bound substrate and bound intermediate at the enzyme active site (K_{int}) could only be estimated from binding constants for the intermediate analogue equilenin. To calculate K_{int} , it is necessary that the reaction of the intermediate (**2**) with the enzyme show saturation kinetics (18), which is not observed for either F101A or F101L. We reasoned that, since the D38E mutant exhibits saturation kinetics upon reaction with **2** (18), the double mutants D38E/F101A and D38E/F101L might also. This expectation was realized, and the complete free energy profiles for these mutants were determined.

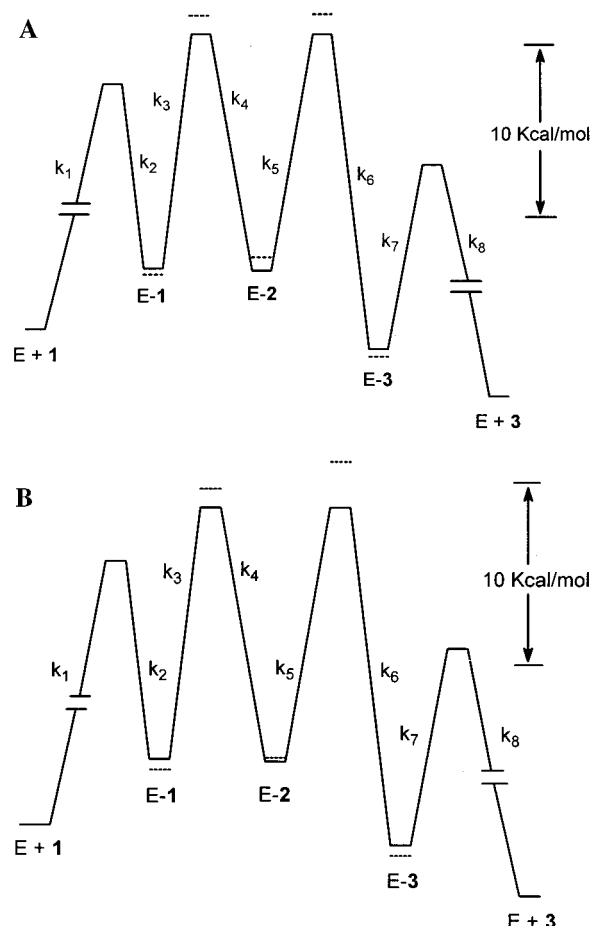


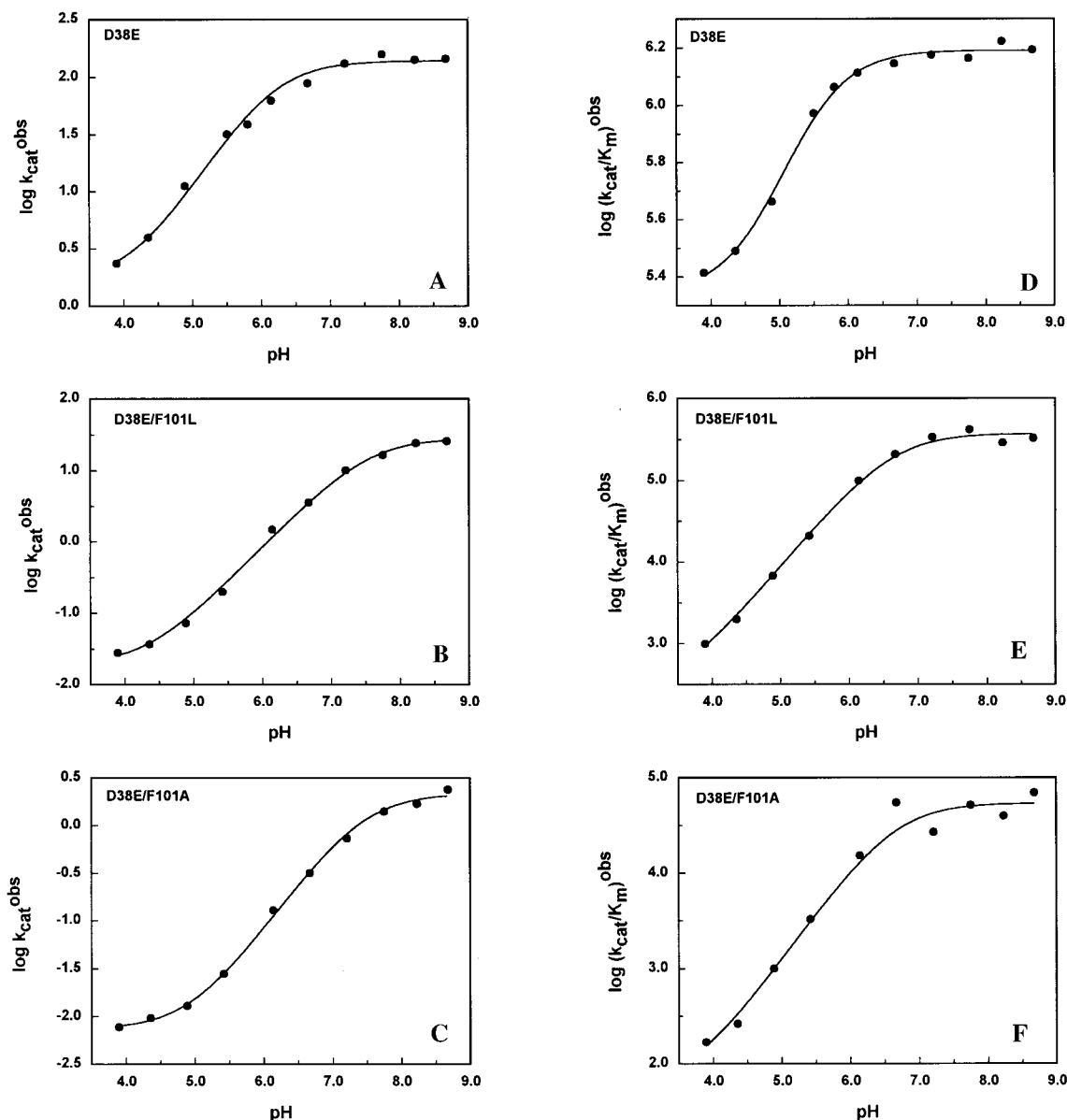
FIGURE 2: Free energy profiles for the isomerization of 5-androstene-3,17-dione to 4-androstene-3,17-dione catalyzed by (A) D38E (—) and D38E/F101L (---); and by (B) D38E (—) and D38E/F101A (---) in 330 mM potassium phosphate buffer and 3.3% MeOH, pH 7.6, 25.0 °C.

A comparison of the free energy profiles for the D38E/F101L and D38E/F101A mutants with that of the D38E mutant (Figure 2) shows that the effect of the phenyl group of Phe-101 is predominantly on the energies of the transition states. Compared to D38E, the energies of the bound substrate and product are slightly lower by 0.3–0.5 kcal/mol and the energies of the bound intermediate are higher by up to 1 kcal/mol. However, the bound transition states are less stable by 1.0–2.5 kcal/mol. Thus, the charged transition states and intermediate are destabilized relative to substrate when the aromatic residue Phe-101 is replaced by the smaller Leu and Ala residues.

A knowledge of the position of Phe-101 allows a discussion of possible mechanisms for the stabilization of the transition state. The recently determined structure of KSI (11) shows that Phe-101 is located at the bottom of the hydrophobic binding pocket slightly below Asp-99 and Tyr-14. Replacement of Phe-101 with a smaller amino acid (Leu or Ala) generates a cavity in the protein, which may be filled either by water molecules or reorganization of the protein. If there is no conformational change, then the presence of additional water molecules would produce an increase in the local active site polarity in the F101 mutants, as well as the possibility of a hydrogen bonding network involving water, Asp-99, and Tyr-14. The decreased reaction rate (k_{cat}) could be due to several factors. An increased active site polarity

Table 4: Calculated Rate Constants for the D38E-, D38E/F101L-, and D38E/F101A-Catalyzed Isomerization of 5-Androstene-3,17-dione to 4-Androstene-3,17-dione^a

D38E ^b		D38E/F101L		D38E/F101A	
rate constant	ΔG^\ddagger (kcal/mol)	rate constant	ΔG^\ddagger (kcal/mol)	rate constant	ΔG^\ddagger (kcal/mol)
$k_1 = 8.6 \times 10^8 \text{ M}^{-1} \text{ s}^{-1}$		$k_1 = 8.6 \times 10^8 \text{ M}^{-1} \text{ s}^{-1}$		$k_1 = 8.6 \times 10^8 \text{ M}^{-1} \text{ s}^{-1}$	
$k_2 = 6.6 \times 10^4 \text{ s}^{-1}$	10.9	$k_2 = 4.1 \times 10^4 \text{ s}^{-1}$	11.1	$k_2 = 2.8 \times 10^4 \text{ s}^{-1}$	11.5
$k_3 = 420 \text{ s}^{-1}$	13.9	$k_3 = 43 \text{ s}^{-1}$	15.3	$k_3 = 26 \text{ s}^{-1}$	15.6
$k_4 = 320 \text{ s}^{-1}$	14.0	$k_4 = 245 \text{ s}^{-1}$	14.3	$k_4 = 75 \text{ s}^{-1}$	15.0
$k_5 = 330 \text{ s}^{-1}$	14.0	$k_5 = 256 \text{ s}^{-1}$	14.3	$k_5 = 6.3 \text{ s}^{-1}$	16.5
$k_6 = 0.11 \text{ s}^{-1}$	18.7	$k_6 = 1.4 \times 10^2 \text{ s}^{-1}$	20.3	$k_6 = 5.9 \times 10^{-4} \text{ s}^{-1}$	22.0
$k_7 = 6.6 \times 10^4 \text{ s}^{-1}$	10.9	$k_7 = 5.2 \times 10^4 \text{ s}^{-1}$	11.2	$k_7 = 2.8 \times 10^4 \text{ s}^{-1}$	11.5
$k_8 = 8.6 \times 10^8 \text{ M}^{-1} \text{ s}^{-1}$		$k_8 = 8.6 \times 10^8 \text{ M}^{-1} \text{ s}^{-1}$		$k_8 = 8.6 \times 10^8 \text{ M}^{-1} \text{ s}^{-1}$	

^a Potassium phosphate buffer, 330 mM, and 3.3% MeOH, pH 7.6, 25.0 °C. ^b Reference 18.FIGURE 3: Plots of $\log(k_{\text{cat}})_{\text{obs}}$ and $(k_{\text{cat}}/K_m)_{\text{obs}}$ for the isomerization of 5-androstene-3,17-dione to 4-androstene-3,17-dione catalyzed by D38E, D38E/F101L, and D38E/F101A as a function of pH. The curves are theoretical, based on eqs 1 and 2 and the parameters given in Table 5.

might affect the rate due to a difference in the extent of charge delocalization in the reactant, the transition states, and the intermediate dienolate (Scheme 1). In the enzyme–substrate complex, the negative charge is spread out over two oxygens in the carboxylate group of Asp-38, whereas in the intermediate the charge is delocalized from O-3 to

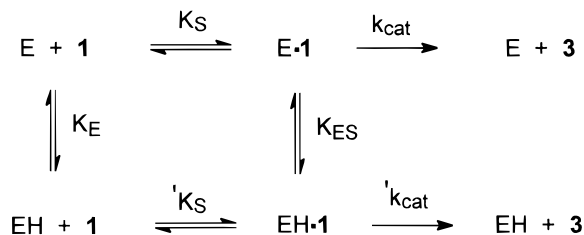
C-6. In the transition states, the charge is further delocalized over both the steroid and the Asp carboxylate. As the polarity of the active site is increased, the intermediate and transition state(s) become less stable relative to the enzyme–substrate complex, and the observed reaction rate decreases. The effect is somewhat greater on the transition states, as

Table 5: pK_a Values for the Free Enzyme (pK_E) and the Enzyme–Substrate Complex (pK_{ES}) with Limiting Rate Constants^a

KSI	pK_E	pK_{ES}	k_{cat}/K_m ($M^{-1} s^{-1}$)	k_{cat}'/K_m' ($M^{-1} s^{-1}$)	k_{cat} (s^{-1})	k_{cat}' (s^{-1})
D38E	5.5	6.1	$(1.55 \pm 0.03) \times 10^6$	$(2.2 \pm 0.1) \times 10^5$	139 ± 9	1.6 ± 0.4
D38E/F101L	6.6	7.5	$(3.7 \pm 0.3) \times 10^5$	250 ± 160	28 ± 3	0.019 ± 0.003
D38E/F101A	6.6	7.4	$(5 \pm 1) \times 10^4$	58 ± 37	2.2 ± 0.2	0.0074 ± 0.0006

^a MeOH, 3.3%, pH 7.0, 25.0 °C.

Scheme 4



their charge is more delocalized than that of the intermediate.³

A hydrogen bonding network between one or two water molecules and Asp-99 and Tyr-14 could also explain the lower activity of the F101 mutants. Hydrogen bonding to either Asp-99 or Tyr-14 by water might make these residues less able to stabilize the incipient dienolate ion, since hydrogen bonds to the dienolate would likely require disruption of hydrogen bonds to water. An alternative explanation may be found in the proposal of Shan et al. (23), who postulate that enzymatic catalysis may be a result of a greater strengthening of hydrogen bonds that accompanies charge rearrangement in nonpolar environments than in polar ones. Thus, the strengthening of the hydrogen bonds from Asp-99 and Tyr-14, which accompanies conversion of **1** to **2**, would be greater in the more hydrophobic environment provided by Phe-101. A similar explanation for the decreased activity of the F101 mutants of KSI has been offered by Kim et al. (24), based upon the crystal structure of the KSI from *P. putida*. They argue that replacement of Phe-101 by water molecules would lower the pK_a of Asp-99 and increase the polarity of the active site, thus decreasing the strength of the hydrogen bonds between the catalytic groups and the dienolate ion.

Variation of Rate with pH. In our previous investigation of the pH dependence of wild-type KSI (4), only slight deviations from a simple titration curve were observed at low pH for plots of either k_{cat} or k_{cat}/K_m vs pH for the nonspecific substrate 5(10)-estrene-3,17-dione. For specific (sticky) substrates, a more complex pH-rate profile was observed. These results were interpreted in terms of ionization of a single catalytically active base (Asp-38), with no activity under conditions where this group is protonated. No dependence of the rate of isomerization on the ionization of a group with $pK_a > 9$ could be observed due to enzyme instability at high pH, although a group of high pK_a had previously been postulated to be important (25).

Since the D38E single and double mutants are substantially less active than WT, chemical steps rather than diffusion processes should be rate-limiting, so that simple titration curves are to be expected (26). However, these pH-rate profiles show considerable residual activity at low pH, and

the analysis must include a term in protonated enzyme. In all three cases, the activity at low pH is significant, as determined from k_{cat} (0.07–1% of the high-pH activity). In addition, there is a perturbation of the observed pK_a by about 1 unit to higher values for each of the double mutants compared to D38E, for both the free enzyme (k_{cat}/K_m plots) and the enzyme–substrate complex (k_{cat} plots).

Although significant residual activity due to protonated enzyme at low pH has not been observed for WT, Holman and Benisek (27) found that the activity does not drop to zero at low pH for both the D38E and D38C mutants. Our results with the D38E mutant differ somewhat from those of Holman and Benisek in that we do not see a diminution of rate at high pH (>8.0), but we do observe the same residual activity at low pH and we obtain similar values for k_{cat} and k_{cat}/K_m . The increase in pK_a for the D38E/F101X mutants, relative to D38E itself, is also puzzling. The phenyl ring of Phe-101 is about 5–8 Å from the carboxylic acid moiety of Glu-38 in this enzyme and, thus, would not be expected to exert any appreciable direct effect on the acidity of this group. Possibly, there is a hydrogen bonding network between Asp-99 and/or Tyr-14 that includes residue 38. Modification of one or more of these hydrogen bonds by mutation of Phe-101 could affect the pK_a of the carboxylate at position 38.

ACKNOWLEDGMENT

We thank Dr. Richard Wolf for a gift of *E. coli* strain NF3079.

REFERENCES

- Pollack, R. M., Bantia, S., Bounds, P. L., and Bevins, C. L. (1989) In *The Chemistry of Enones* (Patai, S., and Rappoport, Z., Eds.) pp 559–597, Wiley, New York.
- Creighton, D. C., and Murthy, N. S. R. K. (1990) In *The Enzymes*, Vol. XIX, pp 323–421, Academic Press, New York.
- Schwab, J. M., and Henderson, B. S. (1990) *Chem. Rev.* 90, 1203–1245.
- Pollack, R. M., Bantia, S., Bounds, P. L., and Koffman, B. M. (1986) *Biochemistry* 25, 1905–1911.
- Kuliopulos, A., Mildvan, A. S., Shortle, D., and Talalay, P. (1989) *Biochemistry* 28, 149–159.
- Benisek, W. F., Ogez, J. R., and Smith, S. B. (1980) *Ann. N.Y. Acad. Sci.* 346, 115–130.
- Bounds, P. L., and Pollack, R. M. (1987) *Biochemistry* 26, 2263–2269.
- Kuliopulos, A., Talalay, P., and Mildvan, A. S. (1990) *Biochemistry* 29, 10271–10280.
- Zeng, B., Bounds, P. L., Steiner, R. F., and Pollack, R. M. (1992) *Biochemistry* 31, 1521–1528.
- Zhao, Q., Mildvan, A. S., and Talalay, P. (1995) *Biochemistry* 34, 426–434.
- Wu, Z. R., Ebrahimian, S., Zawrotny, M. Z., Thornburg, L. D., Perez-Alvarado, G. C., Brothers, P., Pollack, R. M., and Summers, M. F. (1997) *Science* 276, 415–418.
- Hawkinson, D. C., Eames, T. C. M., and Pollack, R. M. (1991) *Biochemistry* 30, 10849–10858.
- Hawkinson, D. C., Pollack, R. M., and Ambulos, N. P. (1994) *Biochemistry* 33, 12172–12183.

³ It is important to note that we are only interpreting the difference in energies of these species. Absolute energies are also affected by other interactions that may be invariant for all species.

14. Zeng, B., and Pollack, R. M. (1991) *J. Am. Chem. Soc.* **113**, 3838–3842.
15. Brothers, P. N., Blotny, G., Qi, L., and Pollack, R. M. (1995) *Biochemistry* **34**, 15453–15458.
16. Sambrook, J., Fritsch, E. F., and Maniatis, T. (1989) *Molecular Cloning: A Laboratory Manual*, 2nd ed., Cold Spring Harbor Laboratory Press, Cold Spring Harbor, NY.
17. Zawrotny, M. E., Ambulos, N. P., Lovett, P. S., and Pollack, R. M. (1991) *J. Am. Chem. Soc.* **113**, 5890–5892.
18. Zawrotny, M. E., and Pollack, R. M. (1994) *Biochemistry* **33**, 13896–13902.
19. Benson, A. M., Suruda, A. J., and Talalay, P. (1975) *J. Biol. Chem.* **250**, 276–280.
20. Kawahara, F. S., Wang, S., and Talalay, P. (1962) *J. Biol. Chem.* **237**, 1500–1506.
21. Barshop, B. A., Wrenn, R. F., and Frieden, C. (1983) *Anal. Biochem.* **130**, 134–145.
22. Frieden, C. (1993) *Trends Biochem. Sci.* **18**, 58–60.
23. Shan, S., and Herschlag, D. (1996) *Proc. Natl. Acad. Sci. U.S.A.* **93**, 14474–14479.
24. Kim, S. W., Cha, S.-S., Cho, H.-S., Kim, J.-S., Ha, N.-C., Cho, M.-J., Joo, S., Kim, K. K., Choi, K. Y., and Oh, B.-H. (1997) *Biochemistry* **36**, 14030–14036.
25. Weintraub, H., Vincent, R., and Baulieu, E.-E. (1970) *Eur. J. Biochem.* **12**, 217–221.
26. Cleland, W. W. (1977) *Adv. Enzymol. Relat. Areas Mol. Biol.* **45**, 273–388.
27. Holman, C. M., and Benisek, W. F. (1995) *Biochemistry* **34**, 14245–14253.

BI972745W